OPEN ACCESS
Fractals, Vol. 30, No. 1 (2022) 2240010 (22 pages)

DOI: 10.1142/S0218348X22400102

THEORETICAL STUDY OF MHD MAXWELL FLUID WITH COMBINED EFFECT OF HEAT AND MASS TRANSFER VIA LOCAL AND NONLOCAL TIME DERIVATIVES

MUHAMMAD BILAL RIAZ
Department of Mathematics
University of Management and Technology
C-II Johar Town, Lahore 54770, Pakistan
Bilalsehole@gmail.com

FAHD JARAD*
Department of Mathematics
Faculty of Arts and Sciences
Cankaya University, Etimesgut Ankara, Turkey
Department of Medical Research
China Medical University Hospital
China Medical University, Taichung Taiwan
fahd@cankaya.edu.tr

DUMITRU BALEANU
Department of Mathematics
Cankaya University, Turkey
Institute of Space Sciences, Magurele
Bucharest, 077125, Romania
dumitru.baleanu@gmail.com

*Corresponding author.

MARYAM ASGIR
Department of Mathematics
Government College University Lahore
maryam.asghar90@gmail.com

Received December 16, 2020
Accepted May 30, 2021
Published September 3, 2021

Abstract

This study highlights the combined effect of heat and mass transfer on MHD Maxwell fluid under time-dependent generalized boundary conditions for velocity, temperature, and concentration. The classical calculus due to the fact that it is assumed as the instant rate of change of the output when the input level changes. Therefore, it is not able to include the previous state of the system called the memory effect. But in the fractional calculus (FC), the rate of change is affected by all points of the considered interval, so it can incorporate the previous history/memory effects of any system. Due to this reason, we applied the modern definition of fractional derivatives (local and nonlocals kernels). Here, the order of fractional derivative will be treated as an index of memory. The exact and semi-analytical solutions are obtained using the integral transform and inversion algorithm. Several important properties of different parameters are analyzed by graphs. Interesting results are revealed by this investigation due to their vast applications in engineering and applied sciences.

Keywords: Memory Effect; MHD; Free Convection; Integral Transform; Fractional Time Derivatives; Local and Nonlocal Kernels; Algorithm.

1. INTRODUCTION

The complexity of the artificial and natural phenomenon description failure with classical calculus leads to the idea of fractional calculus (FC) as there were many aspects of the natural phenomenon which classical calculus fails to capture. The emergence of the field of FC gained much popularity due to its dealing with nonlinear complex systems. Lately, it has been observed as an effective tool that is helpful in physical concept generalization. It has many applications in mechanical engineering, electrical engineering field, food industry,[1] chemical engineering, economics, biomedical, robotics,[2] signal processing,[3] fluid dynamics,[4] etc. Here, we are concerned with the application of FC in fluid dynamics. In fluid dynamics, viscoelastic materials were widely studied with fractional derivative (FD) models. One of the important viscoelastic fluids is Maxwell fluid and has many implementations in the discipline of engineering and science.[5] Jamil *et al.*,[6,7] Khan *et al.*,[8] Vieru and Rauf,[9,10] Fetecau *et al.*,[11,13] contributed much in the studies of Maxwell fluid which address the behavior of fluid relaxation time on the boundary layer.

The study of heat transport accompanied by mass in fluid flows recently attracted many researchers. The application of the fractional approach in this area opens new insights into their behavior in fluid flow and their properties. Heat transmission from radiators, heaters, electric devices, transmission lines, etc., was studied by Ghoshdastidar.[14] Khan *et al.*,[15] wrote the paper on the analysis of heat dissipation of combined convective flow of Maxwell fluid on the vertical oscillating plate. Application of FD in heat transfer phenomenon was discussed by Asjad *et al.*,[16] Imran *et al.*,[17] and many others[18–20] used the FD approach to analyze the heat and mass transfer phenomenon in different fluids with imposed distinct boundary conditions. Vieru[20] studied the convection free flow of incompressible viscous fluid with Newtonian heating and analysis of the diffusion of mass under the consideration of chemical reaction.

The solution of velocity, temperature, and concentration is obtained by Laplace transform (LT) and the solution is expressed in the term of Robotnov–Hartley and Wright functions. Heat and mass transfer rates are also discussed.

Over the last 30 years, FD/FC has captivated numerous researchers after recognition of the fact that in comparison to the classical derivatives, FDs are more reliable operators to model the real-world physical phenomenons. In dynamical problems, fractional-order models/modeling is receiving rapid popularity nowadays. The mathematical modeling of many physical and engineering models based on the idea of FC exhibits highly precise and accurate experimental results as compared to the models based on conventional calculus. For example, the fractional results of rate and differential types fluids have a great resemblance with the results obtained experimentally. Tan *et al.*,[23] studied the generalized second-grade fluid and learned the analytic solution of time-dependent Couette flow. Khan *et al.*,[24] found the exact solution for the unsteady generalized second-grade fluid motion. Imran *et al.*,[25] did the comprehensive fractional CF and ABC study of the convection in MHD viscous fluid with imposed generalized boundary conditions. He studied the time-dependent free convective flow of incompressible Newtonian fluid past over a slanted plate immersed in a porous medium with varying boundary conditions of temperature and concentration. Riaz *et al.*,[26] learned the view of local and nonlocal differential operators of Maxwell fluid in heat and mass transfer study. They consider the Maxwell fluid and investigate the heat and mass transfer with the integer-order, Caputo(C), Caputo–Fabrizio (CF), and Atangana–Baleanu–Caputo (ABC) approach and present their comparison. Some further investigation of fluid flows and their properties equipped with FD is established in the literature.[12,21,22,27–29]

Applications of the combined effect of heat and mass transfer in engineering, applied sciences, and FC since they are connected to the historical data (memory effect). Memory effect in FC means the occurrence of the process depends not only on the present state but also on the past history of the process. FC can remember the prior effects of the input to calculate the current value of the output motivate us to investigate the time-dependent natural convection flow of MHD Maxwell fluid. New definitions of non-integer order derivatives C, CF, and ABC are implemented to model the equations in terms of PDE. The dimensionless concentration, temperature, and velocity profiles with generalized boundary conditions are concluded by LT. The different functions for the generalized boundary conditions are discussed to see their applications in science and engineering. Comparative analysis of the solutions of the considered problem with C, CF, and ABC under the effects of different pertinent parameters is discussed here and illustrated graphically.

2. MATHEMATICAL STATEMENT OF THE PROBLEM

The transport phenomenon of in-compressible MHD Maxwell fluid on an arbitrary plate is discussed here. The plate is considered along the x-$axis$ where the normal acting on the plate is χ-$axis$. In source, the fluid and plate both are at static and temperature is θ'_∞, concentration is Φ'_∞. At time $t = 0^+$, the transfer of heat from plate to fluid raises the temperature of fluid to $\theta'_\infty + \theta'_w h'(t')$ and concentration $\Phi'_\infty + \phi'_w g'(t')$ where $f'(t'), h'(t')$ and $g'(t')$ are piecewise continuous functions. With supposition, the velocity, temperature, and concentration are a function of χ and t, the governing equation for the description of fluid flow are[30,35]

$$\begin{aligned}(1+\lambda'\partial_{t'})\partial_{t'}v'(\chi',t') &= \nu\partial_{\chi'\chi'}v'(\chi',t') + gB_T(1+\lambda'\partial_{t'})(\theta'-\theta'_\infty)\\ &\quad + gB_C(1+\lambda'\partial_{t'})(\Phi'-\Phi'_\infty)\\ &\quad - \frac{\sigma {B_0}^2}{\rho}(1+\lambda'\partial_{t'})v'(\chi',t'), \end{aligned} \tag{1}$$

$$\rho C_p\partial_{t'}\theta'(\chi',t') = K\partial_{\chi'\chi'}\theta'(\chi',t') - S'(\theta'-\theta'_\infty), \tag{2}$$

$$\partial_{t'}\Phi'(\chi',t') = D\partial_{\chi'\chi'}\Phi'(\chi',t') - K_{c'}(\Phi'-\Phi'_\infty). \tag{3}$$

Different parameters description is given in Table 1. The relevant initial and boundary conditions are

$$v'(\chi',t') = 0, \quad \theta'(\chi',t') = \theta'_\infty, \quad \Phi'(\chi',t') = \Phi'_\infty, \tag{4}$$

$\chi' \geq 0$, $t' \leq 0$, and for $t' > 0$

$$\begin{aligned} v'(\chi',t') &= v_0 f'(t'), \quad \theta'(\chi',t') = \theta'_\infty + \theta'_w h'(t'),\\ \Phi'(\chi',t') &= \Phi'_\infty + \Phi'_w g'(t'), \quad \chi' = 0, \end{aligned}$$

Table 1 Nomenclature.

Symbol	Quantity
u	Fluid velocity
B_0	Applied magnetic field value
q	LT parameter
D	Diffusivity of mass
B_T	Heat expansion coefficient
B_C	Coefficient of concentration expansion
K	Heat conductivity
ρ	Density of fluid
λ	Relaxation time
σ	Electric conductivity coefficient
μ	Viscosity of fluid (dynamic)
υ	Viscosity of fluid (kinematic)
c_p	Specific heat
S	Heat source parameter
K_c	Chemical reaction coefficient
g	Gravitational acceleration
S_C	Schmidt number
M	Parameter of magnetic field
P_r	Prandtl number
G_T	Grashof number (thermal)
G_C	Grashof number (mass)

$$v'(\chi', t') \to 0, \quad \theta'(\chi', t') \to \theta'_\infty,$$
$$\Phi'(\chi', t') \to \Phi'_\infty, \quad \chi' \to \infty. \tag{5}$$

For dimensionless problem, we use the following relations

$$t = \frac{{v_0}^2}{\nu} t', \quad \chi = \frac{v_0}{\nu}\chi', \quad S_c = \frac{\nu}{D}, \quad K_c = \frac{\nu}{{v_0}^2} K'_c,$$
$$\lambda = \frac{{v_0}^2}{\nu}\lambda', \quad v' = v_0 v, \quad \Phi = \frac{\Phi' - \Phi'_\infty}{\Phi'_w}, \tag{6}$$
$$\theta = \frac{\theta' - \theta'_\infty}{\theta'_w}, \quad S = \frac{\nu}{\rho C_p {v_0}^2 S'}, \quad P_r = \frac{\mu C_p}{K},$$
$$K'_p = \frac{{v_0}^2}{\nu^2} K_p, \quad G_c = \frac{gB_C/\nu}{{v_0}^3}\Phi'_w, \tag{7}$$
$$G_T = \frac{gB_T\nu}{{v_0}^3}\theta'_w, \quad M = \frac{\sigma {B_0}^2 \nu}{\rho {v_0}^2}, \quad f = \frac{\nu}{{v_o}^2} f',$$
$$g = \frac{\nu}{v_o^2} g', h = \frac{\nu}{{v_o}^2} h'. \tag{8}$$

After dropping the $'$, the dimensionless system of equations is as follows:

$$(1 + \lambda\partial_t)\partial_t v(\chi, t) = \partial_{\chi\chi} v(\chi, t) + G_T(1 + \lambda\partial_t)\theta(\chi, t) + G_C(1 + \lambda\partial_t)\Phi(\chi, t) - M(1 + \lambda\partial_t)v(\chi, t), \tag{9}$$

$$\partial_t \theta(\chi, t) = \frac{1}{P_r}\partial_{\chi\chi}\theta(\chi, t) - S\theta(\chi, t), \tag{10}$$

$$\partial_t \Phi(\chi, t) = \frac{1}{S_c}\partial_{\chi\chi}\Phi(\chi, t) - K_c\Phi(\chi, t). \tag{11}$$

For the fluid flow, the suitable initial and boundary conditions are stated as follows:

$$v(\chi, t) = 0, \quad \theta(\chi, t) = 0, \quad \Phi(\chi, t) = 0, \quad \text{at } t = 0, \tag{12}$$

$$v(\chi, t) = f(t), \quad \theta(\chi, t) = h(t), \quad \Phi(\chi, t) = g(t), \quad \text{at } \chi = 0, \tag{13}$$

$$v(\chi, t) \to 0, \quad \theta(\chi, t) \to 0, \quad \Phi(\chi, t) \to 0 \quad \text{as } \chi \to \infty. \tag{14}$$

To develop the fractional derivative models, the order-one time derivative is replaced with C, CF, and AB fractional derivative of order $\alpha \in (0, 1)$.

2.1. Caputo Fractional Formulation of the Problem

Equations (9)–(11) take the form after applying the time fractional C derivative

$$(1 + \lambda {}^C D_t^\alpha)\partial_t v(\chi, t) = \partial_{\chi\chi} v(\chi, t) + G_T(1 + \lambda {}^C D_t^\alpha)\theta(\chi, t) + G_C(1 + \lambda {}^C D_t^\alpha)\Phi(\chi, t) - M(1 + \lambda {}^C D_t^\alpha)v(\chi, t), \tag{15}$$

$${}^C D_t^\alpha \theta(\chi, t) = \frac{1}{P_r}\partial_{\chi\chi}\theta(\chi, t) - S\theta(\chi, t), \tag{16}$$

$${}^C D_t^\alpha \Phi(\chi, t) = \frac{1}{S_c}\partial_{\chi\chi}\Phi(\chi, t) - K_c\Phi(\chi, t), \tag{17}$$

and the time fractional C derivative for $\alpha \in (0, 1)$

$${}^C D_t^\alpha f(\chi, t) = \frac{1}{\Gamma(1 - \alpha)} \int_0^t (t - \vartheta)^{-\alpha} f'(\chi, \vartheta) d\vartheta. \tag{18}$$

The LT of C time derivative

$$L({}^C D_t^\alpha f(\chi, t)) = s^\alpha L(f(\chi, t)) - s^{\alpha-1} f(\chi, 0). \tag{19}$$

2.2. Caputo–Fabrizio Formulation of the Problem

CF time derivative transforms Eqs. (9)–(11)

$$(1+\lambda^{\mathrm{CF}}D_t^{\alpha})\partial_t v(\chi,t) = \partial_{\chi\chi}v(\chi,t) + (1+\lambda^{\mathrm{CF}}D_t^{\alpha}) \times \{G_T\theta(\chi,t) + G_C\Phi(\chi,t) - Mv(\chi,t)\}, \tag{20}$$

$${}^{\mathrm{CF}}D_t^{\alpha}\theta(\chi,t) = \frac{1}{P_r}\partial_{\chi\chi}\theta(\chi,t) - S\theta(\chi,t), \tag{21}$$

$${}^{\mathrm{CF}}D_t^{\alpha}\Phi(\chi,t) = \frac{1}{S_c}\partial_{\chi\chi}\Phi(\chi,t) - K_c\Phi(\chi,t), \tag{22}$$

and the time fractional CF derivative for $\alpha \in (0,1)$

$${}^{\mathrm{CF}}D_t^{\alpha}f(\chi,t) = \frac{1}{1-\alpha}\int_0^t e^{(\frac{-\alpha(t-\vartheta)}{1-\alpha})}f'(\chi,\vartheta)d\vartheta. \tag{23}$$

The transformation of time-fractional CF derivative by LT appears

$$L({}^{\mathrm{CF}}D_t^{\alpha}f(\chi,t)) = \frac{sL(f(\chi,t)) - f(\chi,0)}{s(1-\alpha)+\alpha}. \tag{24}$$

2.3. Atangana–Baleanu Formulation of the Problem

The implementation of ABC fractional time derivative transforms Eqs. (9)–(11) into

$$(1+\lambda^{\mathrm{ABC}}D_t^{\alpha})\partial_t v(\chi,t) = \partial_{\chi\chi}v(\chi,t) + (1+\lambda^{\mathrm{ABC}}D_t^{\alpha}) \times \{G_T\theta(\chi,t) + G_C\Phi(\chi,t) - Mv(\chi,t)\}, \tag{25}$$

$${}^{\mathrm{ABC}}D_t^{\alpha}\theta(\chi,t) = \frac{1}{P_r}\partial_{\chi\chi}\theta(\chi,t) - S\theta(\chi,t), \tag{26}$$

$${}^{\mathrm{ABC}}D_t^{\alpha}\Phi(\chi,t) = \frac{1}{S_c}\partial_{\chi\chi}\Phi(\chi,t) - K_c\Phi(\chi,t), \tag{27}$$

where the ABC time fractional derivative for $\alpha \in (0,1)$

$${}^{\mathrm{ABC}}D_t^{\alpha}f(\chi,t) = \frac{1}{1-\alpha}\int_0^t E_{\alpha}\left(\frac{-\alpha(t-\vartheta)^{\alpha}}{1-\alpha}\right) \times f'(\chi,\vartheta)d\vartheta, \tag{28}$$

where E_{α} is a Mittag–Leffler function. LT of ABC time derivative emerges

$$L({}^{\mathrm{ABC}}D_t^{\alpha}f(\chi,t)) = \frac{s^{\alpha}L(f(\chi,t)) - s^{\alpha-1}f(\chi,0)}{s^{\alpha}(1-\alpha)+\alpha}. \tag{29}$$

3. SOLUTIONS

3.1. Caputo Fractional Time Derivative

Concentration

The application of the LT in Eq. (17) with the use of concerned initial condition from Eq. (12) transforms into

$$\partial_{\chi\chi}\bar{\Phi}(\chi,p) - S_c(K_c+p^{\alpha})\bar{\Phi}(\chi,p) = 0. \tag{30}$$

The obtained solution of Eq. (30) appears

$$\bar{\Phi}(\chi,p) = G(p)e^{-\chi\sqrt{S_c(K_c+p^{\alpha})}}. \tag{31}$$

Temperature

Implementation of the LT in Eq. (16) and using the corresponding initial condition from Eq. (12), the differential equation formed

$$\partial_{\chi\chi}\bar{\theta}(\chi,p) - P_r(S+p^{\alpha})\bar{\theta}(\chi,p) = 0. \tag{32}$$

The obtained solution of the above equation seems as

$$\bar{\theta}(\chi,p) = H(p)e^{-\chi\sqrt{P_r(S+p^{\alpha})}}. \tag{33}$$

Velocity

Employing the LT in Eq. (9) and embedding the corresponding initial condition from Eq. (12)

$$\partial_{\chi\chi}\bar{v}(\chi,p) - ((1+\lambda p^{\alpha})(p+M))\bar{v}(\chi,p) = -G_T(1+\lambda p^{\alpha})\bar{\theta}(\chi,p) - G_c(1+\lambda p^{\alpha})\bar{\Phi}(\chi,p). \tag{34}$$

Substituting the expression of $\bar{\Phi}(\chi,p)$, $\bar{\theta}(\chi,p)$ from Eqs. (31) and (33), respectively, and utilizing the corresponding boundary conditions from Eqs. (13) and (14) gives the solution

$$\bar{v}(\chi,p) = F(p)e^{-\chi\sqrt{(p+M)(1+\lambda p^{\alpha})}} + \frac{G_T H(p)(1+\lambda p^{\alpha})\left(e^{-\chi\sqrt{(p+M)(1+\lambda p^{\alpha})}} - e^{-\chi\sqrt{P_r(S+p^{\alpha})}}\right)}{(P_r(S+p^{\alpha}) - (1+\lambda p^{\alpha})(p+M))} + \frac{G_c G(p)(1+\lambda p^{\alpha})\left(e^{-\chi\sqrt{(p+M)(1+\lambda p^{\alpha})}} - e^{-\chi\sqrt{S_c(K_c+p^{\alpha})}}\right)}{(S_c(K_c+p^{\alpha}) - (1+\lambda p^{\alpha})(p+M))}. \tag{35}$$

3.2. Caputo–Fabrizio Time Derivative

Concentration

For the solution, implementing the LT in Eq. (22) with the use of the corresponding conditions, we arrive at

$$\bar{\Phi}(\chi,p)=G(p)e^{-\chi\sqrt{\frac{S_c(K_c(\gamma p+\alpha)+p)}{\gamma p+\alpha}}}, \tag{36}$$

where $\gamma=1-\alpha$.

Temperature

The solution of temperature by applying the LT in Eq. (21) is given as

$$\bar{\theta}(\chi,p)=H(p)e^{-\chi\sqrt{\frac{P_r(S(\gamma p+\alpha)+p)}{\gamma p+\alpha}}}, \tag{37}$$

where $\gamma=1-\alpha$.

Velocity

Operating the LT in Eq. (20) and making use of the corresponding initial condition Eq. (12)

$$\begin{aligned}\partial_{\chi\chi}\bar{v}(\chi,p)-\left((p+M)\left(\frac{\xi p+\alpha}{\gamma p+\alpha}\right)\right)\bar{v}(\chi,p)\\ =-G_T\left(\frac{\xi p+\alpha}{\gamma p+\alpha}\right)\bar{\theta}(\chi,p)\\ -G_c\left(\frac{\xi p+\alpha}{\gamma p+\alpha}\right)\bar{\Phi}(\chi,p),\end{aligned} \tag{38}$$

where $\gamma=1-\alpha,\xi=\gamma+\lambda$.

The solution of the above differential equation after embedding the value of $\bar{\Phi}(\chi,p)$, $\bar{\theta}(\chi,p)$, from Eqs. (36) and (37), respectively, and implementing the corresponding boundary conditions

$$\begin{aligned}\bar{v}(\chi,p)=F(p)e^{-\chi\sqrt{(p+M)(\frac{\xi p+\alpha}{\gamma p+\alpha})}}\\ +\frac{G_TH(p)(\xi p+\alpha)}{(P_r(\zeta p+S\alpha)-(\xi p+\alpha)(p+M))}\\ \times\left(e^{-\chi\sqrt{(p+M)(\frac{\xi p+\alpha}{\gamma p+\alpha})}}-e^{-\chi\sqrt{P_r(\frac{\zeta p+S\alpha}{\gamma p+\alpha})}}\right)\\ +\frac{G_cG(p)(\xi p+\alpha)}{(S_c(\eta p+K_c\alpha)-(\xi p+\alpha)(p+M))}\\ \times\left(e^{-\chi\sqrt{(p+M)(\frac{\xi p+\alpha}{\gamma p+\alpha})}}-e^{-\chi\sqrt{S_c(\frac{\eta p+K_c\alpha}{\gamma p+\alpha})}}\right),\end{aligned} \tag{39}$$

where $\zeta=S\gamma+1,\eta=Kc\gamma+1$.

3.3. Atangana–Baleanu Fractional Time Derivative

Concentration

The LT implementation in Eq. (27) with the corresponding initial and boundary conditions, the solution for the concentration

$$\bar{\Phi}(\chi,p)=G(p)e^{-\chi\sqrt{\frac{S_c(\eta p^\alpha+K_c\alpha)}{\gamma p^\alpha+\alpha}}}, \tag{40}$$

where $\gamma=1-\alpha,\eta=Kc\gamma+1$.

Temperature

Implementing the LT in Eq. (26) and practicing the transformed initial and boundary conditions, the solution is

$$\bar{\theta}(\chi,p)=H(p)e^{-\chi\sqrt{\frac{P_r(\zeta p^\alpha+S\alpha)+p)}{\gamma p^\alpha+\alpha}}}, \tag{41}$$

where $\gamma=1-\alpha,\xi=\gamma+\lambda$.

Velocity

Employing the LT in Eq. (25) and imposing the corresponding initial condition from Eq. (12)

$$\begin{aligned}\partial_{\chi\chi}\bar{v}(\chi,p)-\left((p+M)\left(\frac{\xi p^\alpha+\alpha}{\gamma p^\alpha+\alpha}\right)\right)\bar{v}(\chi,p)\\ =-G_T\left(\frac{\xi p^\alpha+\alpha}{\gamma p^\alpha+\alpha}\right)\bar{\theta}(\chi,p)\\ -G_c\left(\frac{\xi p^\alpha+\alpha}{\gamma p^\alpha+\alpha}\right)\bar{\Phi}(\chi,p),\end{aligned} \tag{42}$$

where $\gamma=1-\alpha,\xi=\gamma+\lambda$.

The value of $\bar{\Phi}(\chi,p)$, $\bar{\theta}(\chi,p)$ from Eqs. (40) and (41), respectively, and use of the boundary conditions transforms the solution into

$$\begin{aligned}\bar{v}(\chi,p)=F(p)e^{-\chi\sqrt{(p+M)\left(\frac{\xi P^\alpha+\alpha}{\gamma p^\alpha+\alpha}\right)}}\\ G_TH(p)(\xi p^\alpha+\alpha)\left(e^{-\chi\sqrt{(p+M)(\frac{\xi p^\alpha+\alpha}{\gamma p^\alpha+\alpha})}}\right.\\ \left.-e^{-\chi\sqrt{P_r(\frac{\zeta p^\alpha+S\alpha}{\gamma p^\alpha+\alpha})}}\right)\\ +\frac{}{(P_r(\zeta p^\alpha+S\alpha)-(\xi p^\alpha+\alpha)(p+M))}\\ G_cG(p)(\xi p^\alpha+\alpha)\left(e^{-\chi\sqrt{(p+M)(\frac{\xi p^\alpha+\alpha}{\gamma p^\alpha+\alpha})}}\right.\\ \left.-e^{-\chi\sqrt{S_c(\frac{\eta p^\alpha+K_c\alpha}{\gamma p^\alpha+\alpha})}}\right)\\ +\frac{}{(S_c(\eta p^\alpha+K_c\alpha)-(\xi p^\alpha+\alpha)(p+M))},\end{aligned} \tag{43}$$

where $\zeta=S\gamma+1,\eta=K_c\gamma+1$.

The Laplace inverse transforms for the solution of velocity, temperature, and concentration attained

by applying Stehfest's and Tzou's numerical algorithms.[31,32] Stehfest's algorithm is defined as

$$\varphi(\chi,t)=\frac{\ln(2)}{t}\sum_{k=1}^{2n}d_j\bar{\varphi}\left(\chi,k,\frac{\ln(2)}{t}\right),$$

where n is a positive integer and

$$d_j=(-1)^{k+n}\times\sum_{i=[\frac{k+1}{2}]}^{\min(k,n)}\frac{i^n(2i)!}{(n-i)!i!(i-1)!(k-i)!(2i-k)!},$$

where the real number integer part is described by $[\cdot]$. The Tzou's numerical algorithm is defined as

$$\varpi(r,t)=\frac{e^{4.7}}{t}\left[\frac{1}{2}\bar{\varpi}\left(r,\frac{4.7}{t}\right)+\mathrm{Re}J_1\right],\quad(44)$$

where $J_1=\{\sum_{j=1}^{N_1}(-1)^j\bar{\varpi}(r,\frac{4.7+k\pi i}{t})\}$, $\mathrm{Re}(\cdot)$ is the real part, the imaginary part is i, and $N_1\gg 1$ represents the natural number.

The above results are obtained for generalized boundary conditions. The different values of the generalized boundary conditions have many applications in the field of applied science and engineering. Here, we consider a few of its applications. The Heaviside function is helpful in engineering problems such as signal processing, control theory, driving/impulsive forces that act shorty, structural loads, etc. The linear function is of important use in chemical, electrical, mechanical, nuclear, biomedical, and chemical engineering. Like, electrical engineers use the linear function to solve the problems of current, voltage, and resistance. In bio-medical engineering, they are used to find the interaction of different medicines and used to estimate the correct dosage of medicine to avoid overdose in patients. To learn about slope, engineers use linear functions to read and understand graphs that show displacement, velocity, and acceleration. They use these functions to analyze data to learn how to design their products to more efficient and reliable. One of the famous application of *sint* in composing the computer music is the application of this function in sound engineering. In architecture, it is helpful to calculate the structural load, ground surface, slope of roofs, etc. In flight engineering, it is used to calculate speed, distance, direction with the speed, and direction of the wind. In civil and mechanical engineering, these functions are used to calculate torque and forces on objects, which help build bridges, girders. In life science engineering, the exponential function is widely used in population growth/decay models. Nuclear engineers use this function in models that describe the radioactive decay phenomenon. In nuclear engineering, some elements under consideration are unstable and emit energy spontaneously and exponential functions help calculate that energy. In basic engineering, it is used to calculate the tensile strength, which determines the amount of stress that a structure can withstand. In aeronautical engineering, it is used to predict how jets, airplanes, and rockets will perform during flight. They help us to predict wave behavior which helps us to calculate potential and kinetic energy and to measure pressure, heat, and airflow. For validation of our results, results are compared with the results already present in the literature. If we choose $h(t)=1$, we will obtain the same results for temperature profile as obtained by Abro *et al.*,[33] for Atangana–Baleanu fractional method. If we choose $g(t)=t$, then we will get the same results for concentration profile as obtained by Iftikhar *et al.*[34] For $\lambda\to 0$, we will get the results for viscous fluid which are already present in the literature. For $\alpha\to 1$, we will get the same results as obtained by Riaz *et al.*[30]

4. RESULTS AND DISCUSSION

Comparative study of unsteady MHD Maxwell fluid for non-integer order derivative C, CF, and ABC is studied here. Physical aspects of fractional parameter α, Prandtl number P_r, Maxwell fluid parameter λ, thermal Grashof number G_T, mass Grashof number G_c, Schmidt number S_c, the magnetic parameter M, heat absorption S, chemical reaction parameter K_c and of time on the solutions for velocity profile, temperature, and concentration profile are discussed and illustrated in graphs.

Figure 1 portrays the increase in non-integer order variable α boosts the fluid velocity at small and large time scales. The boundary layer thickness size increases along with the increase in the fractional parameter α and time. It is clearly shown the velocity for the ABC model is maximum because of the nonlocal kernel as compared to the CF and C models. Results for limiting case $\alpha\to 1$ is calculated and compared with the results found in the literature.[30] Impacts of magnetic parameter M displayed in Fig. 2 depict the velocity decline with the increase of magnetic parameter values. A resistive force arises under the effects of the magnetic field

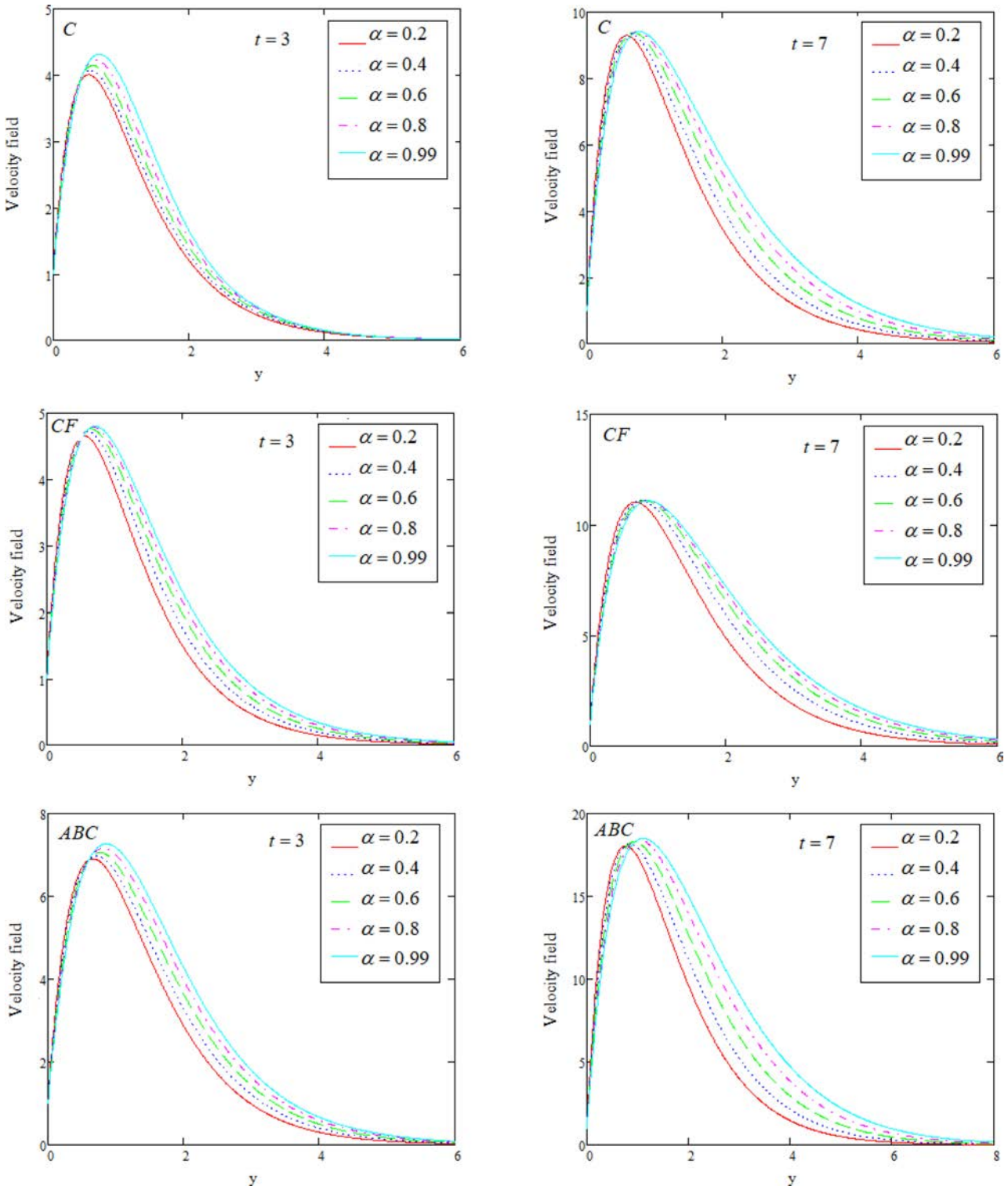

Fig. 1 Comparison of Caputo, Caputo–Fabrizio and ABC velocity portrait for varying of α with $P_r = 7, \lambda = 1.8, S = 0.5, S_c = 0.96, K_c = 0.5, G_T = 5.0, G_C = 8.0, M = 1.5$ and for $f(t) = H(t), g(t) = t, h(t) = sint$.

which delays the motion of fluid in the boundary layer. While comparing between C, CF, and ABC approach, the ABC has more memory effects as compared to others.

In Fig. 3, the study of the effects of G_T on velocity describes the increase in behavior with increment in the G_T. The depiction of G_C on velocity is portrayed in Fig. 4. We can see the rise in velocity with

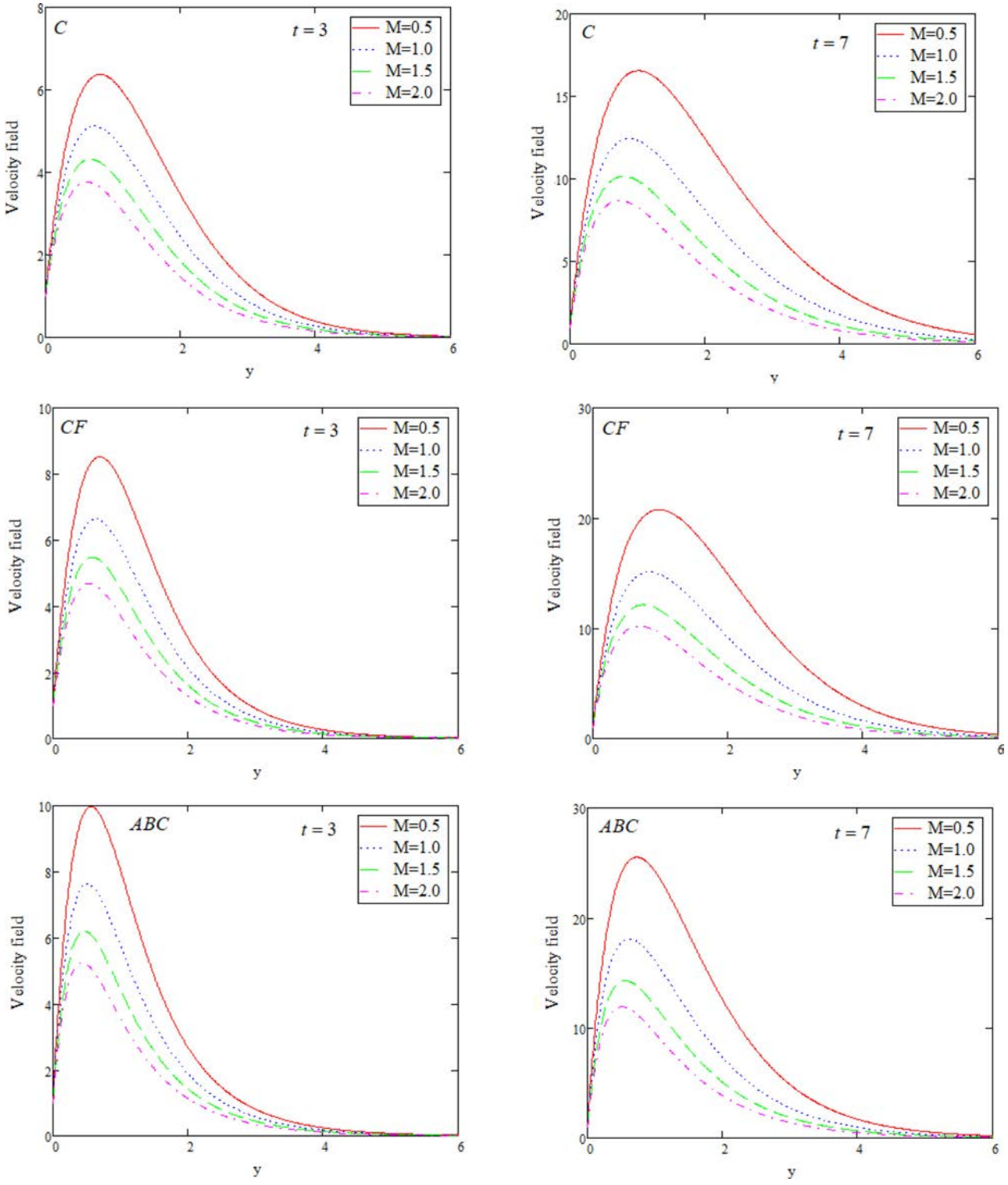

Fig. 2 Comparison of Caputo, Caputo–Fabrizio and ABC velocity portrait for varying of M with $P_r = 7, \lambda = 1.8, S = 0.5, S_c = 0.96, K_c = 0.5, G_T = 5.0, G_C = 8.0, \alpha = 0.6$ and for $f(t) = H(t), g(t) = t, h(t) = sint$.

the rise in the value of G_C. The reason of that buoyancy forces becoming dominant than viscous forces causes the natural convection and accelerates the velocity.

The curve for velocity for the distinct use of the values of the Maxwell fluid parameter λ is plotted in Fig. 5. It is noted the fluid flow increased with the rise in the values of the relaxation parameter.

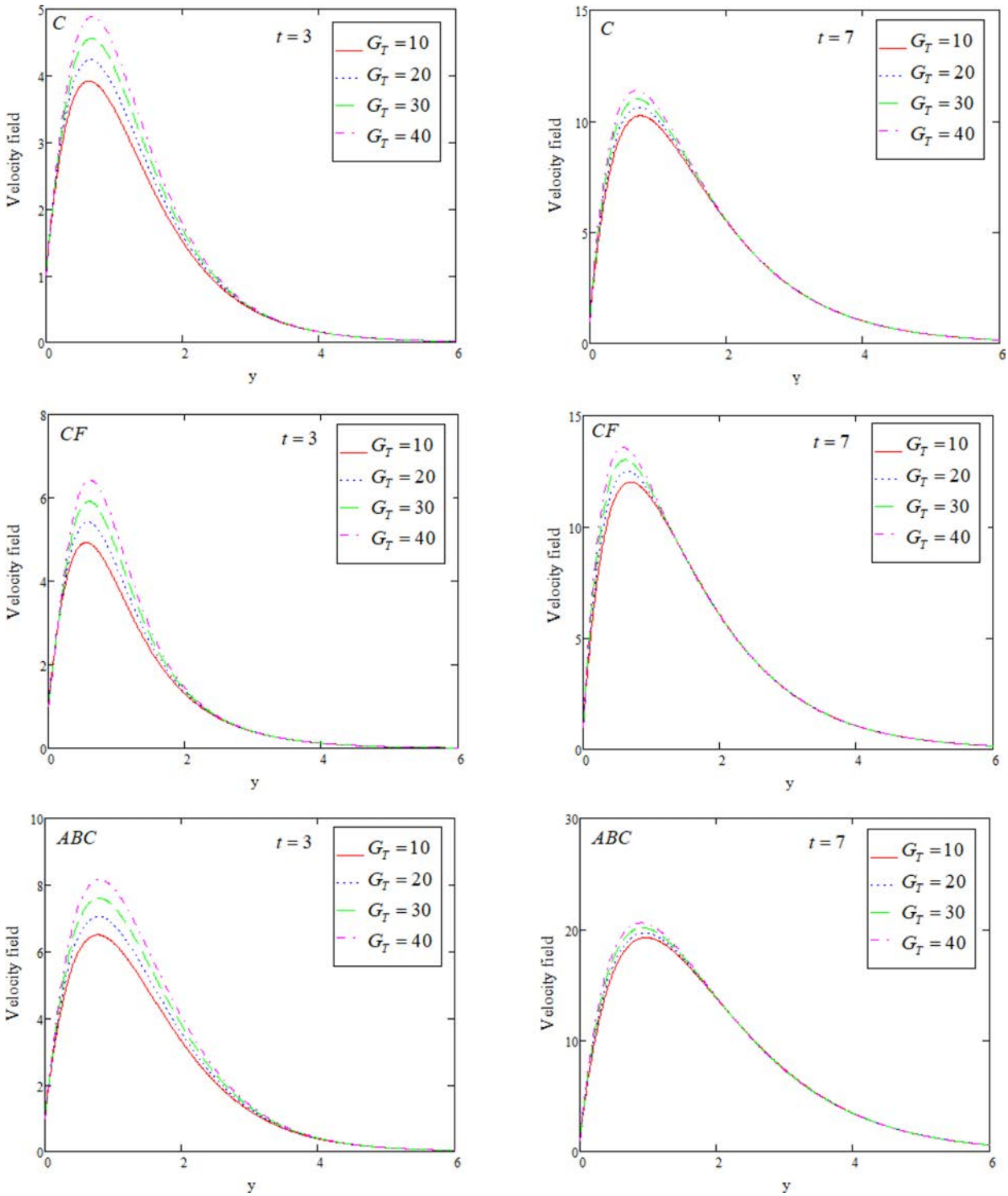

Fig. 3 Comparison of Caputo, Caputo–Fabrizio and ABC velocity portrait for varying of G_T with $P_r = 7, \lambda = 1.8, M = 1.5, S = 0.5, S_c = 0.96, K_c = 0.5, G_C = 8.0, \alpha = 0.6$ and for $f(t) = H(t), g(t) = t, h(t) = sint$.

The reason is, the existence of relaxation parameter increases the speed of fluid flow effectively. ABC velocity profile is larger as compared to C and CF. Figure 6 shows that with the increase in P_r decreases the velocity at different time scales. In fact, the Prandtl number increases, the fluid viscosity increase results in decline in thermal boundary layer thickness and thus velocity. Physically, the Prandtl number defines the correlation between momentum diffusivity and thermal diffusivity. In

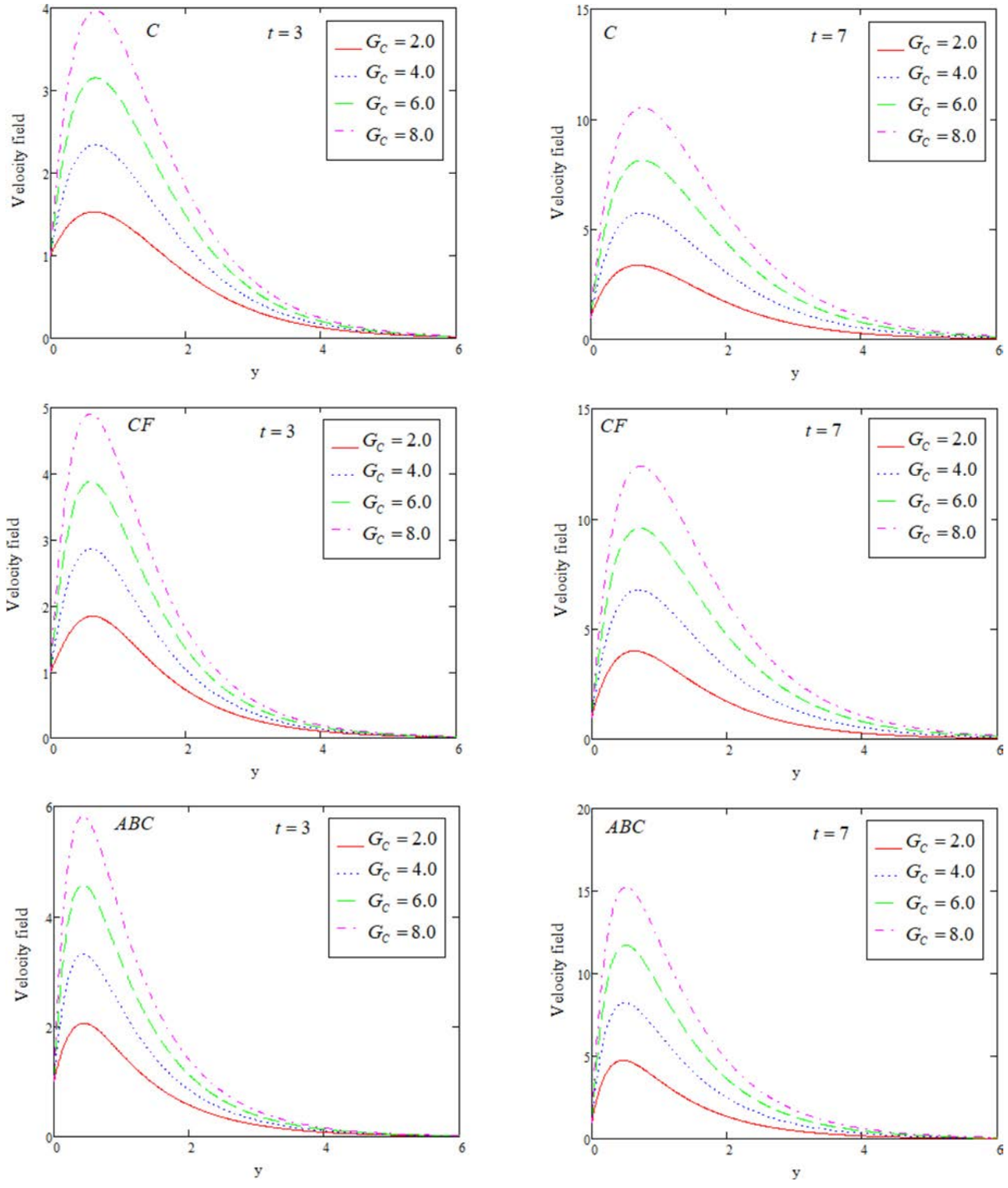

Fig. 4 Comparison of Caputo, Caputo–Fabrizio and ABC velocity portrait for varying of G_C with $P_r = 7, \lambda = 1.8, M = 1.5, S = 0.5, S_c = 0.96, K_c = 0.5, G_T = 5.0, \alpha = 0.6$ and for $f(t) = H(t), g(t) = t, h(t) = sint$.

fact, in the heat transfer phenomenon, the relative thickness of the momentum and thermal boundary layers is controlled by P_r. In Fig. 7, representation of S_C on velocity profile for ABC, CF, and C models is sketched. The ratio of kinematic viscosity and mass diffusivity is defined as the Schmidt number. An increase in it means the fall of mass diffusivity and decrease in the boundary

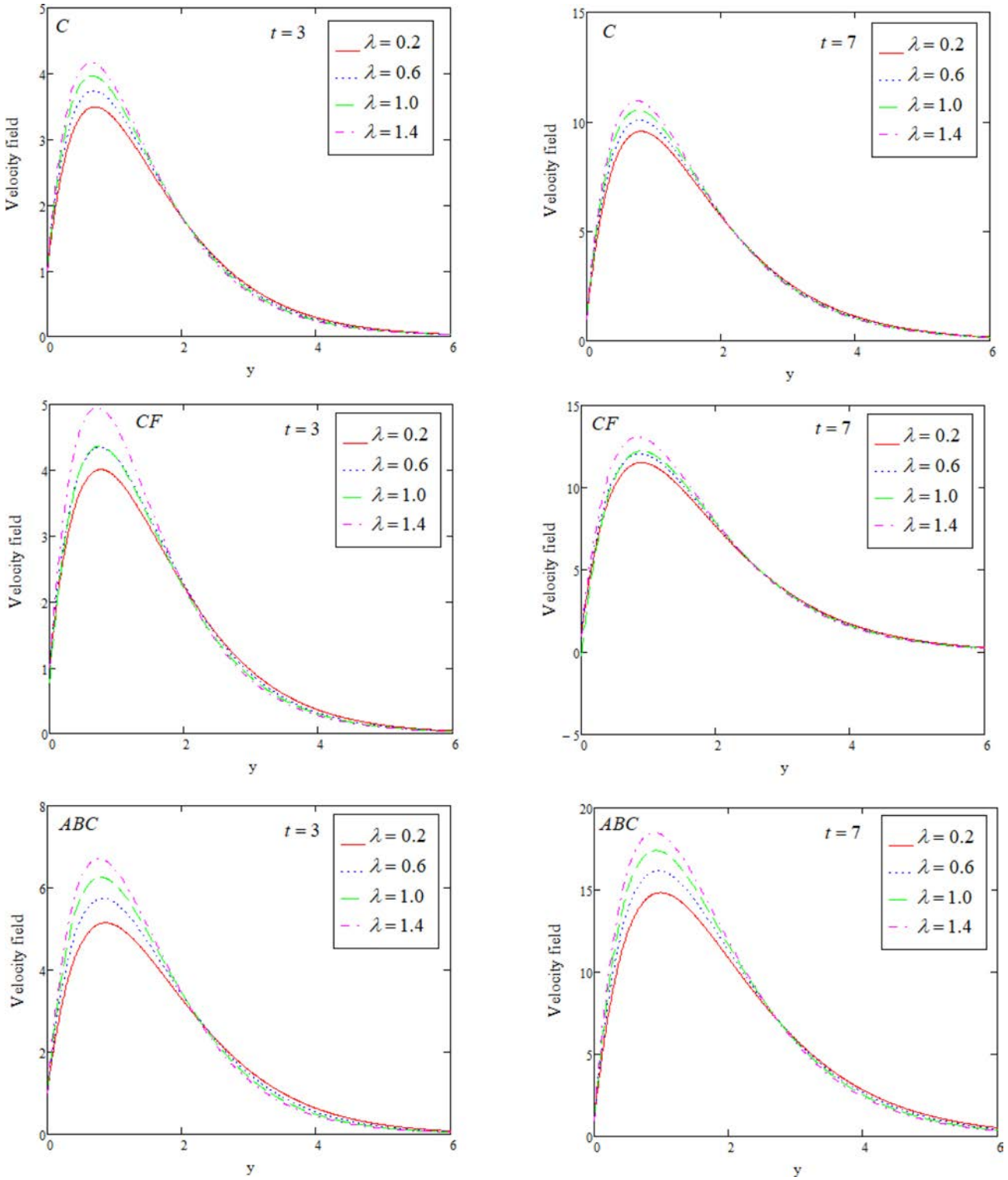

Fig. 5 Comparison of Caputo, Caputo–Fabrizio and ABC velocity portrait for varying of λ with $P_r = 0.71, M = 1.5, S = 0.5, S_c = 0.96, K_c = 0.5, G_T = 5.0, G_C = 8.0, \alpha = 0.6$ and for $f(t) = H(t), g(t) = t, h(t) = sint$.

layer thickness which results in a decrease in the velocity.

The impact of the chemical reaction parameter is the same as of S_C as shown in Fig. 8. The velocity of fluid falls due to a rise in chemical reaction constant. From a physical point of view, the increase in the values of K_c is termed destructive. That is the reason for the decline

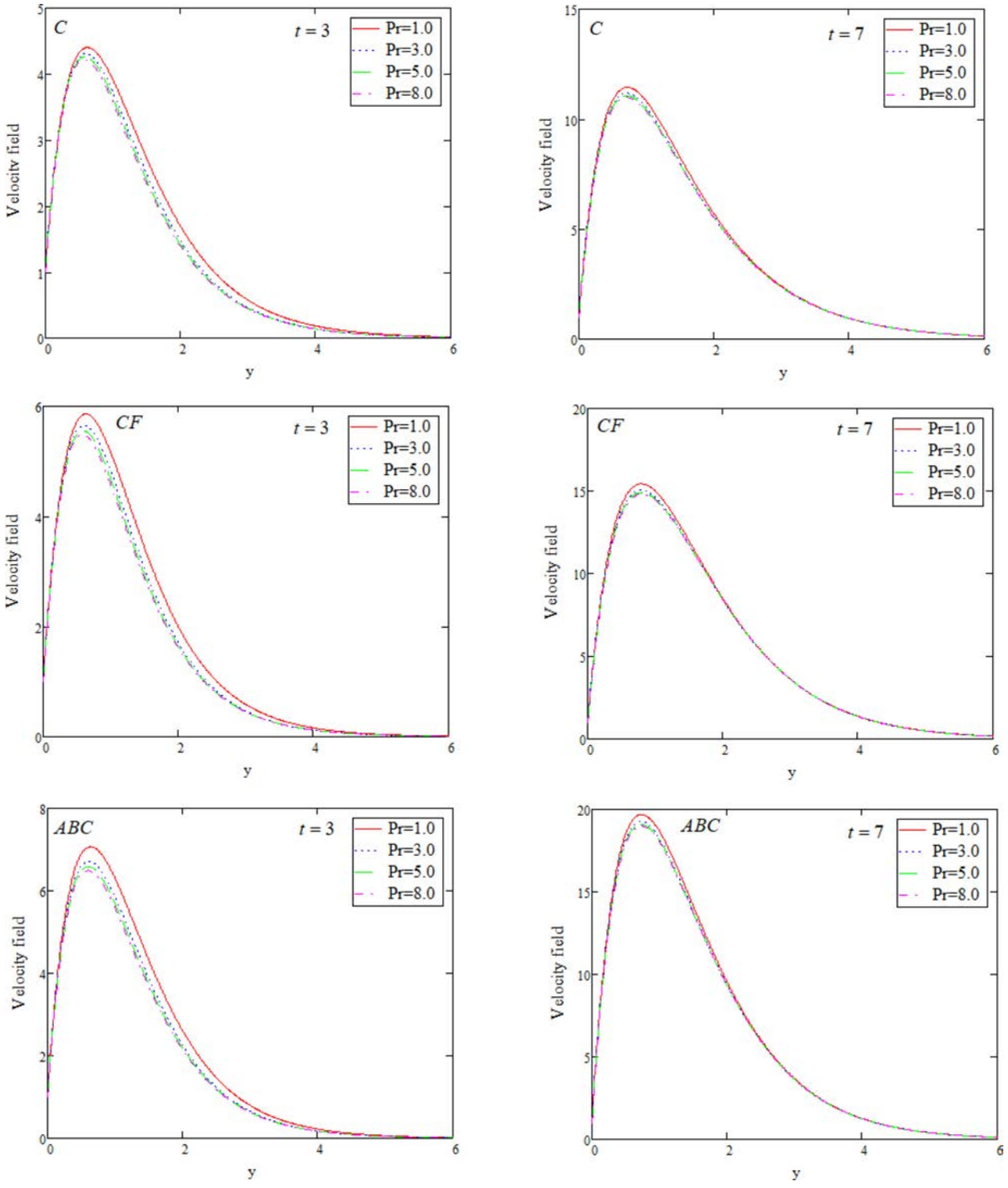

Fig. 6 Comparison of Caputo, Caputo–Fabrizio and ABC velocity portrait for varying of P_r with $\lambda = 2.0, M = 1.5, S = 0.5, S_c = 0.96, K_c = 0.5, G_T = 5.0, G_C = 8.0, \alpha = 0.6$ and for $f(t) = H(t), g(t) = t, h(t) = sint$.

in the velocity of the fluid as K_c increases. The velocity profiles for varying in the values of the heat absorption parameter S are plotted in Fig. 9. It is seen from these curves that the velocity decreases with the increase in the value of parameter S.

The behavior of velocity versus time is plotted in Figs. 10 and 11. In Fig. 10, the transient

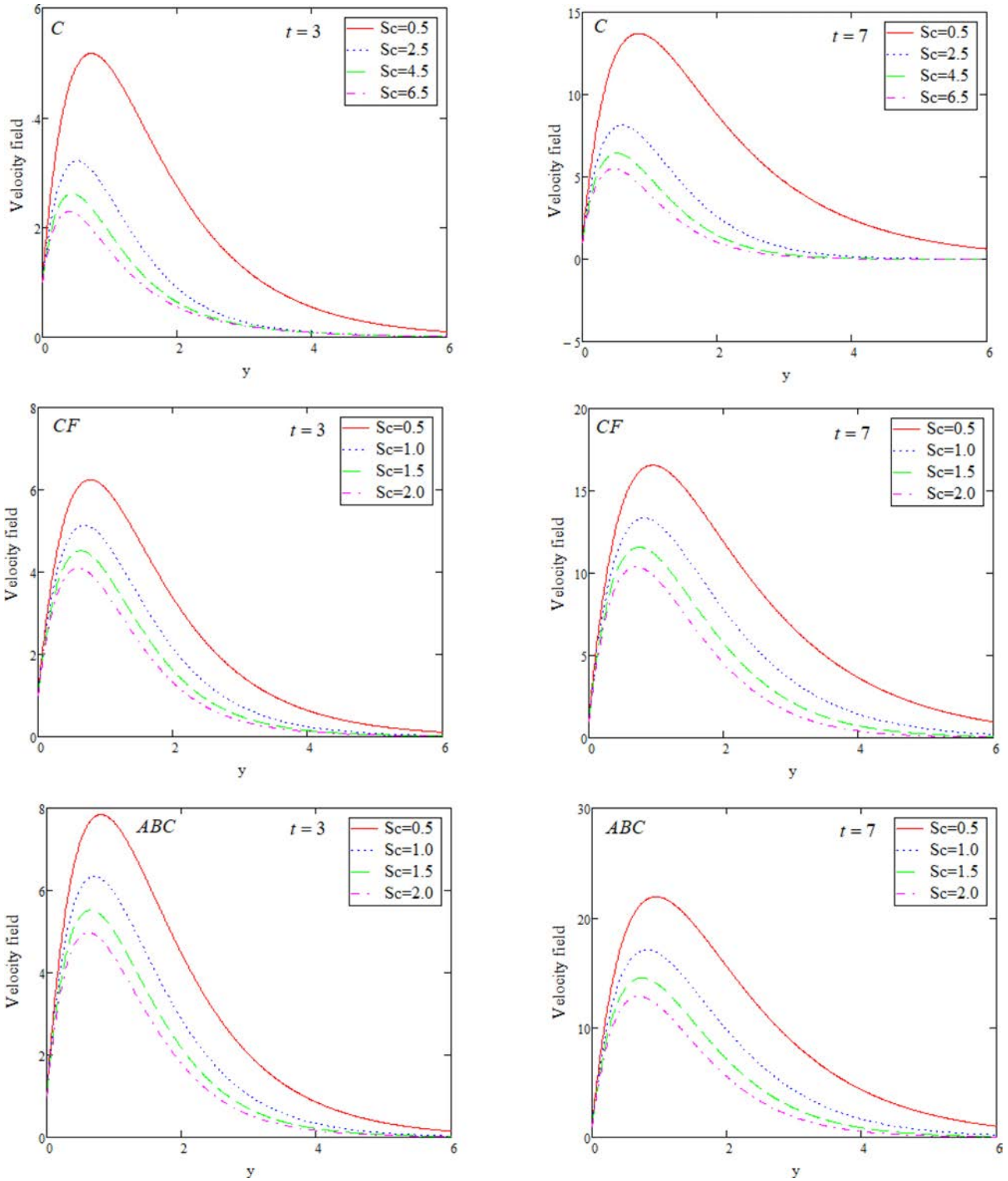

Fig. 7 Comparison of Caputo, Caputo–Fabrizio and ABC velocity portrait for varying of S_c with $\lambda = 1.8, P_r = 0.71, M = 1.5, S = 0.5, K_c = 0.5, G_T = 5.0, G_C = 8.0, \alpha = 0.6$ and for $f(t) = H(t), g(t) = t, h(t) = sint$.

velocity profile is plotted for various values of relaxation parameter λ. It is seen, with an increase in λ, the velocity declines. The same results are obtained for the effects of the magnetic parameter as shown in Fig. 11. The comparative study of three fractional models depicts the ABC model has the highest velocity as compared to CF and C models.

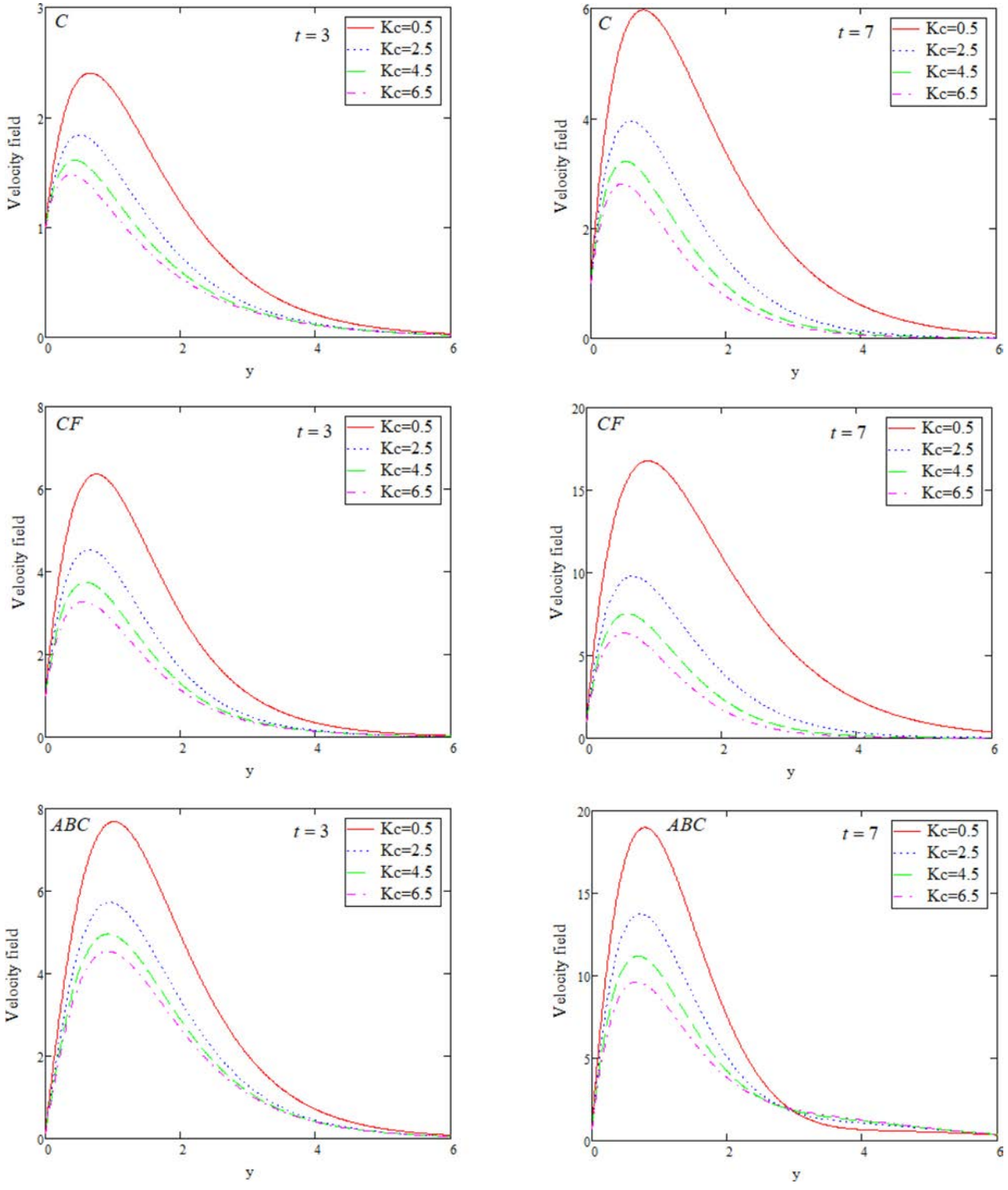

Fig. 8 Comparison of Caputo, Caputo–Fabrizio and ABC velocity portrait for varying of K_c with $\lambda = 1.8, M = 1.5, S = 0.5, S_c = 0.96, P_r = 0.71, G_T = 5.0, G_C = 8.0, \alpha = 0.6$ and for $f(t) = H(t), g(t) = t, h(t) = sint$.

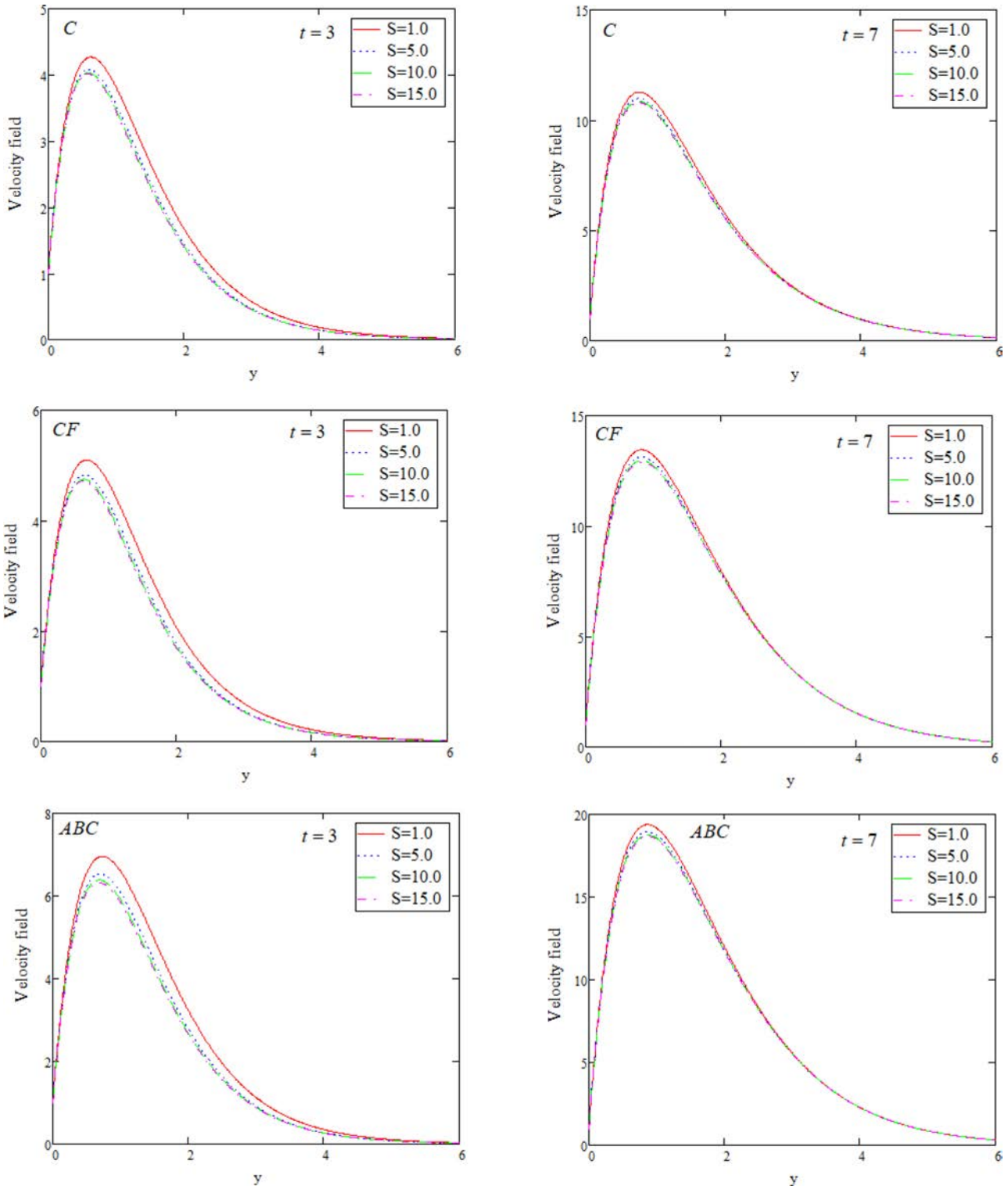

Fig. 9 Comparison of Caputo, Caputo–Fabrizio and ABC velocity portrait for varying of K_c with $\lambda = 1.8, M = 1.5, P_r = 0.71, S_c = 0.96, K_c = 0.5, G_T = 5.0, G_C = 8.0, \alpha = 0.6$ and for $f(t) = H(t), g(t) = t, h(t) = sint$.

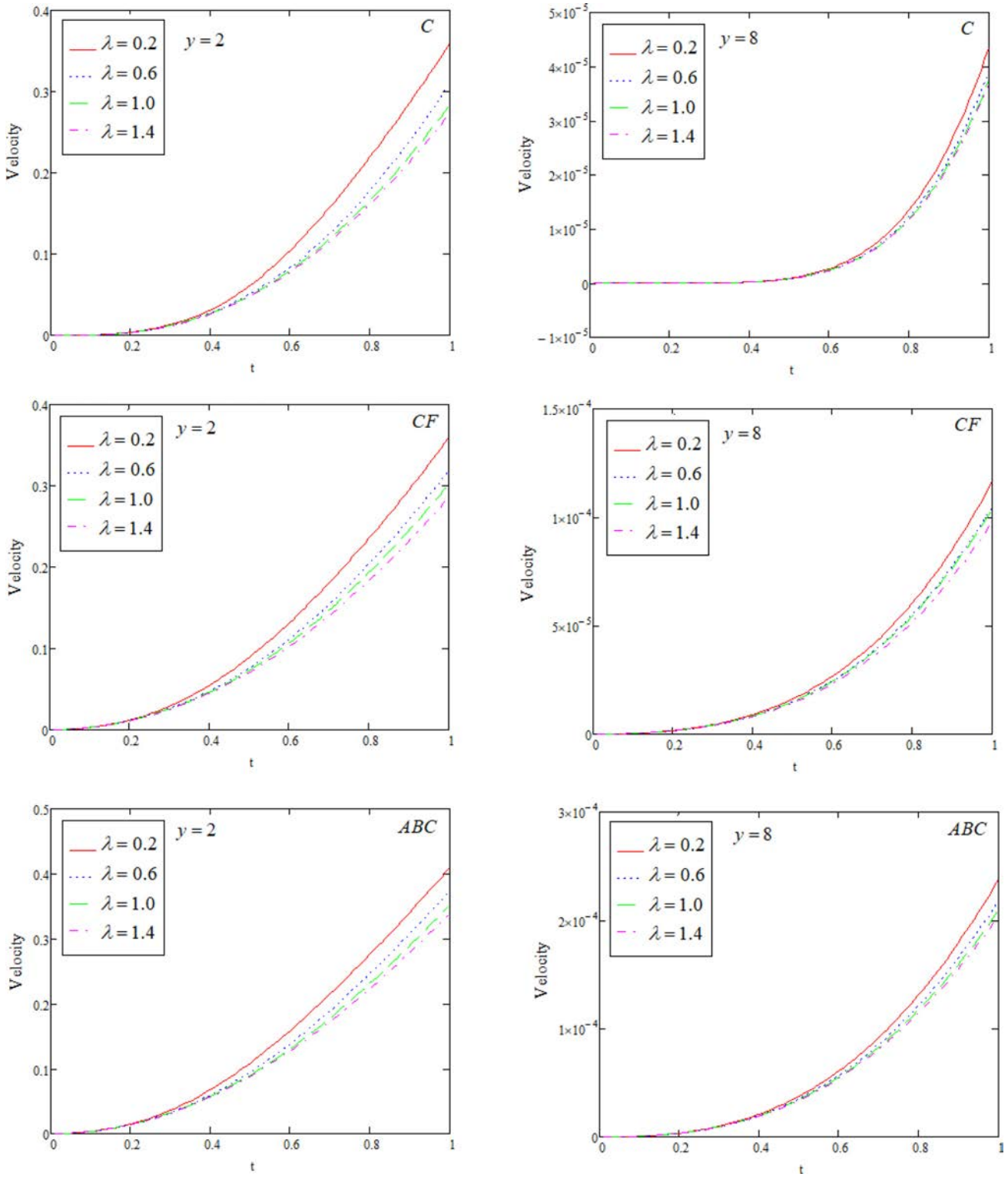

Fig. 10 Comparison of Caputo, Caputo–Fabrizio and ABC transient velocity portrait for varying of λ with $M = 2.0, S = 0.5, P_r = 0.71, S_c = 0.96, K_c = 0.5, G_T = 5.0, G_C = 8.0, \alpha = 0.6$ and for $f(t) = H(t), g(t) = t, h(t) = sint$.

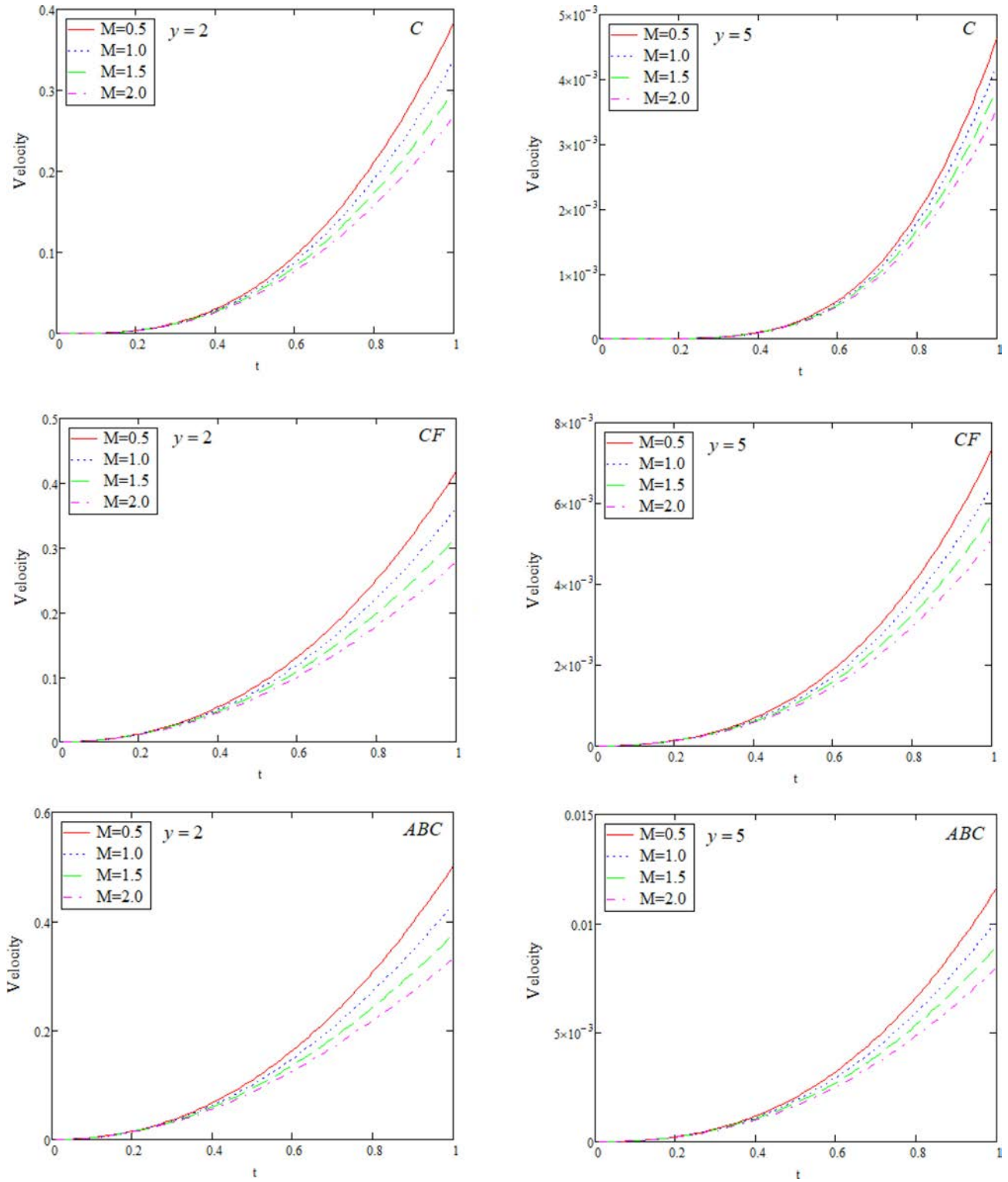

Fig. 11 Comparison of Caputo, Caputo–Fabrizio and ABC transient velocity portrait for varying of M with $\lambda = 1.8, S = 0.5, P_r = 0.71, S_c = 0.96, K_c = 0.5, G_T = 5.0, G_C = 8.0, \alpha = 0.6$ and for $f(t) = H(t), g(t) = t, h(t) = sint$.

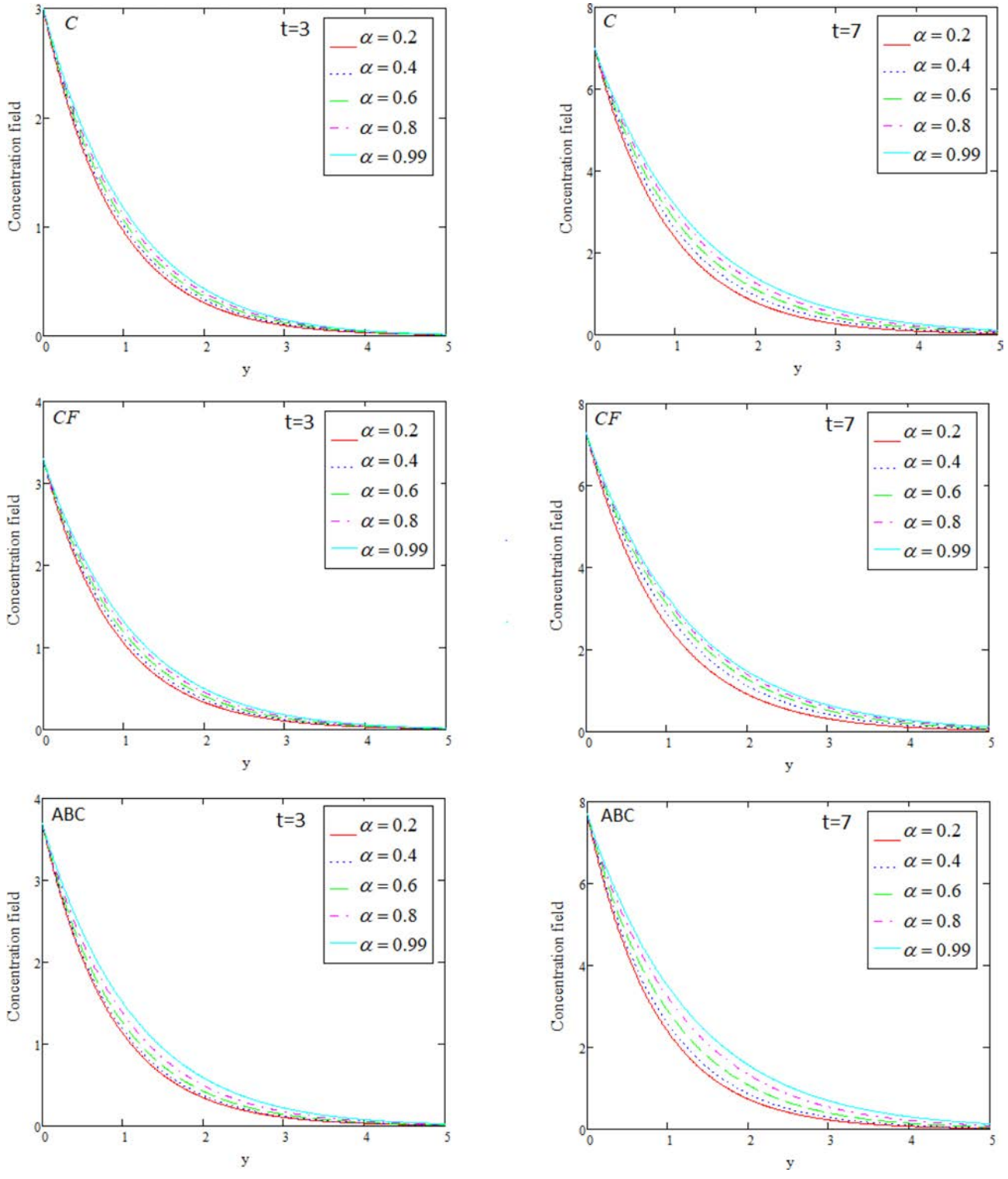

Fig. 12 Comparison of Caputo, Caputo–Fabrizio and ABC concentration portrait for varying of α with $S_c = 0.96, K_c = 0.5$ and for $g(t) = t$.

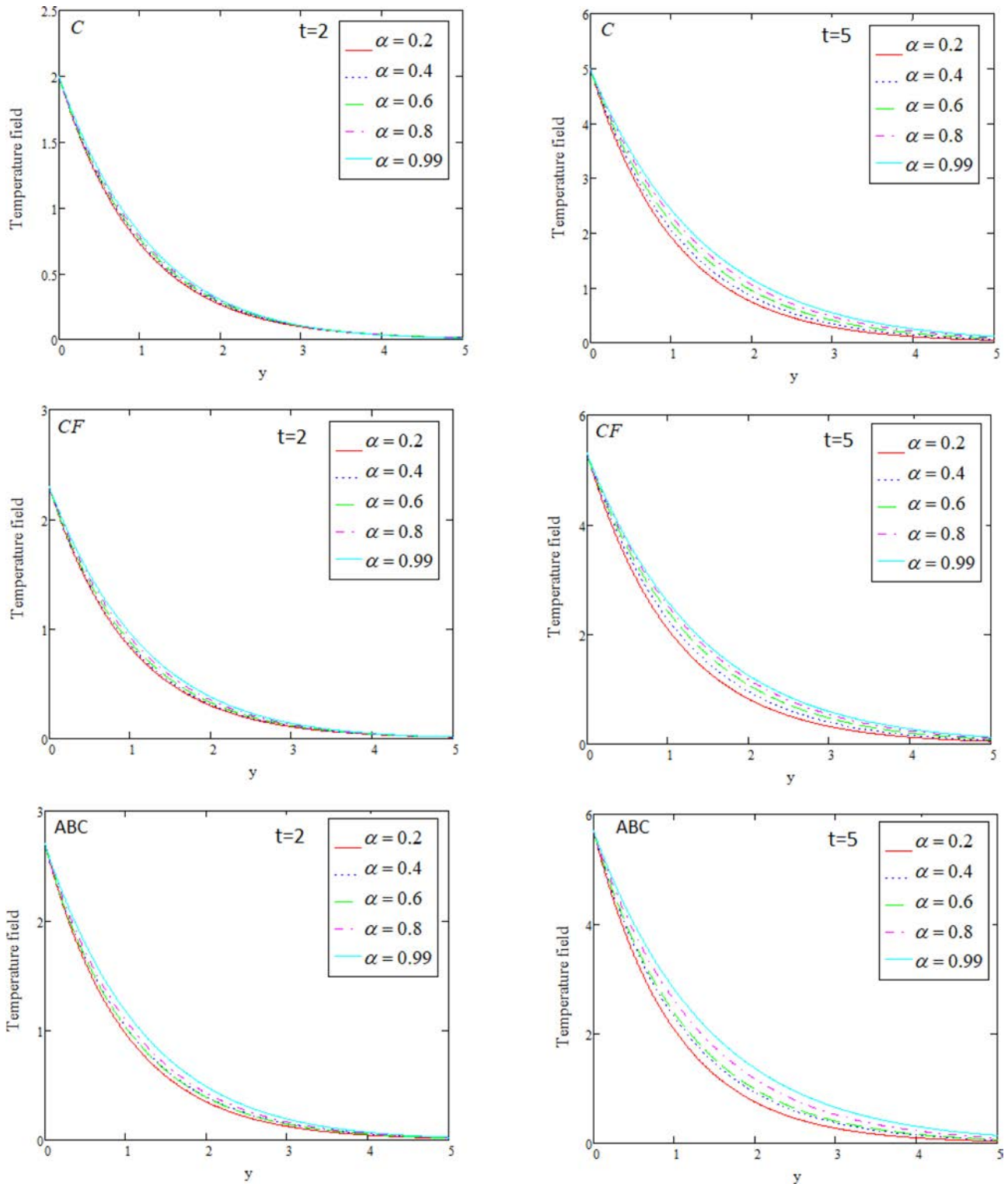

Fig. 13 Comparison of Caputo, Caputo–Fabrizio and ABC temperature portrait for varying of α with $P_r = 0.71, S = 0.5$ and for $h(t) = t$.

behavior of concentration curves for ABC is shown relative to C and CF. The same effects of α on the temperature field are shown in Fig. 13. For $\alpha \to 1$, temperature curves for the fractional-order approach to integer order.

5. CONCLUSIONS

The combined effects of heat and mass transfer on MHD Maxwell fluid are analyzed here. A fractional generalized model of Maxwell fluid was developed by Caputo, Caputo–Fabrizio, and Atangana–Baleanu and solved by the LT method. The exact solution is obtained for dimensionless concentration, temperature, and velocity which satisfied the imposed initial and boundary conditions. Impacts of magnetic parameter, relaxation parameter, thermal Grashof number, Schmidt number, mass Grashof number, Prandtl number, chemical reaction, heat source on motion of the fluid are discussed. Some comparisons have been drawn between C, CF, and ABC. We conclude this paper by the following remarks:

- The fractional parameter α has a consequential impact on the dimensionless velocity, concentration, and temperature fields. The increase in the fractional parameter α increases the boundary layer thickness which increases velocity, concentration, and temperature.
- The velocity decreases with the increase in the Lorentz force due to magnetic field M, the increase in Prandtl number P_r decreases the thermal conductivity results in a decrease in velocity.
- The decrease in thermal buoyancy force due to heat absorption coefficient S drops in molecular diffusivity with the increase in chemical reaction parameter and, increase in momentum diffusivity due to Schmidt number S_c, results in a decrease in velocity of fluid flow.
- The velocity increases with an increase in the buoyancy forces due to an increase in thermal Grashof number G_T, mass Grashof number G_C, and rise in Maxwell fluid parameter λ reduces the viscosity which increases the speed of the fluid flow.
- In sense of comparison, the ABC fractional model is most suited in simulating the functions of velocity, concentration, temperature fields in comparison to CF and C models.
- In a limiting case, when $\alpha \to 1$, the results recovered are of classical generalized Maxwell fluid.

ACKNOWLEDGMENT

The authors are highly thankful and grateful to their respective departments and Universities for supporting and facilitating the research work. This work can be extended for Oldroyd-B, second grade and Jeffery fluids.

REFERENCES

1. F. Ali, F. Ali, N. Ahmad Sheikh, I. Khan and K. S. Nisar, Caputo–Fabrizio fractional derivatives modeling of transient MHD Brinkman nanoliquid: Applications in food technology, *Chaos Solitons Fractals* **131** (2020) 109489.
2. J. A. T. Machado, System modeling and control through fractional-order algorithms, in *Nonlinear Dynamics*, *Chaos*, *Control and Their Applications to Engineering Sciences* Vol. 4 (Springer, 2002), pp. 99–116.
3. H. M. Ozaktas, O. Arikan, M. A. Kutay and G. Bozdagi, Digital computation of the fractional Fourier transform, *IEEE Trans. Signal Process.* **44** (1996) 2141–2150.
4. V. Kulish and J. L. Lage, Application of fractional calculus to fluid mechanics, *J. Fluids Eng.* **124**(3) (2002) 803–806.
5. M. Jamil, K. A. Abro and N. A. Khan, Helices of fractionalized Maxwell fluid, *Nonlinear Eng.* **4** (2015) 191–201.
6. J. M. Fetecau and C. Fetecau, Unsteady flow of viscoelastic fluid between two cylinders using fractional Maxwell model, *Acta Mech. Sin.* **28** (2012) 274–280.
7. M. Jamil, Effects of slip on oscillating fractionalized Maxwell fluid, *Nonlinear Eng.* **5**(1) (2016) 25–36, https://doi.org/10.1515/nleng-2015-0030.
8. I. Khan, F. Ali, S. Ul Haq and S. Shafie, Exact solutions for unsteady MHD oscillatory flow of a Maxwell fluid in a porous medium, *Z. Naturforsch.* **68a** (2013) 635–645 (2013), doi:10.5560/ZNA.2013-00401–11.
9. D. Vieru and A. Rauf, Stokes flows of a Maxwell fluid with wall slip condition, *Can. J. Phys.* **89** (2011) 1061–1071.
10. D. Vieru and A. A. Zafar, Some Couette flows of a Maxwell fluid with wall slip condition, *Appl. Math. Inf. Sci.* **7** (2013) 209–219.
11. C. Fetecau and C. Fetecau, A new exact solution for the flow of a Maxwell fluid past an infinite plate, *Int. J. Nonlinear Mech.* **38** (2003) 423–427.
12. K. Das and S. Jana, Heat and mass transfer effects on unsteady MHD free convection flow near a moving plate in porous medium, *Bull. Soc. Math.* **17** (2010) 15–32.

13. J. Zierep and C. Fetecau, Energetic balance for the Rayleigh–Stokes problem of Maxwell fluid, *Int. J. Eng. Sci.* **45** (2007) 617–627.
14. P. S. Ghoshdastidar, *Heat Transfer* (Oxford University Press, Oxford, UK, 2004).
15. I. Khan, N. A. Shah and L. C. C. Dennis, A scientific report on heat transfer analysis in mixed convection flow of Maxwell fluid over an oscillating vertical plate, *Sci. Rep.* **7** (2017) 40147, https://doi.org/10.1038/srep40147.
16. M. I. Asjad, N. A. Shah, M. Aleem and I. Khan, Heat transfer analysis of fractional second-grade fluid subject to Newtonian heating with Caputo and Caputo–Fabrizio fractional derivatives: A comparison, *Eur. Phys. J. Plus* **132** (2017) 340.
17. M. A. Imran, M. B. Riaz, N. A. Shah and A. A. Zafar, Boundary layer flow of MHD generalized Maxwell fluid over an exponentially accelerated infinite vertical surface with slip and Newtonian heating at the boundary, *Res. Phys.* **8** (2018) 1061–1067.
18. M. A. Imran, I. Khan, M. Ahmad, N. A. Shah and M. Nazar, Heat and mass transport of differential type fluid with non-integer order time-fractional Caputo derivatives, *J. Mol. Liq.* **229** (2017) 67–75.
19. I. Khan, N. A. Shah and D. Vieru, Unsteady flow of generalized Casson fluid with fractional derivative due to an infinite plate, *Eur. Phys. J. Plus* **131** (2016) 10.
20. D. Vieru, C. Fetecau and F. Corina, Time fractional free convection flow near a vertical plate with Newtonian heating and mass discussion, *Int. J. Therm. Sci.* **19** (2015) S85–S98.
21. K. A. Abro, I. Khan and A. Tassaddiq, Application of Atangana–Baleanu fractional derivative to convection flow of MHD Maxwell fluid in a porous medium over a vertical plate, *Math. Model. Nat. Phenom.* **13** (2018) 1.
22. M. Tahir, M. A. Imran, N. Raza, M. Abdullah and M. Aleem, Wall slip and non-integer order derivative effects on the heat transfer flow of Maxwell fluid over an oscillating vertical plate with new definition of fractional Caputo–Fabrizio derivatives, *Res. Phys.* **7** (2017) 1887–1898.
23. W. C. Tan, F. Xian and L. Wei, Exact solution for the unsteady Couette flow of the generalized second grade fluid, *China Sci. Bull.* **47** (2002) 1226–1228.
24. M. Khan, S. Nadeem, T. Hayat and A. M. Siddiqui, Unsteady motions of a generalized second grade fluid, *Math. Comput. Model.* **41** (2005) 629–637.
25. M. A. Imran, M. Aleem, M. B. Riaz, R. Ali and I. Khan, A comprehensive report on convective flow of fractional (ABC) and (CF) MHD viscous fluid subject to generalized boundary conditions, *Chaos Solitons Fractals* **118** (2019) 274–289.
26. M. B. Riaz, A. Atangana and N. Iftikhar, Heat and mass transfer in Maxwell fluid in view of local and nonlocal differential operators, *J. Therm. Anal. Calorim.* **143** (2021) 4313–4329, https://doi.org/10.1007/s10973-020-09383-7.
27. I. Khan, N. A. Shah, Y. Mahsud and D. Vieru, Heat transfer analysis in a Maxwell fluid over an oscillating vertical plate using fractional Caputo–Fabrizio derivatives, *Eur. Phys. J. Plus* **132** (2017) 194.
28. C. Fetecau, A. A. Zafar, D. Vieru and J. Awrejcewicz, Hydromagnetic flow over a moving plate of second grade fluids with time fractional derivatives having non-singular kernel, *Chaos Solitons Fractals* **130** (2020) 109454.
29. J. H. Zhao, L. C. Zheng, X. X. Zhang and F. W. Liu, Unsteady natural convection boundary layer heat transfer of fractional Maxwell viscoelastic fluid over a vertical plate, *Int. J. Heat Mass Transf.* **97** (2016) 760–766.
30. M. B. Riaz, M. Asgir, A. A. Zafar and S. Yao, Combined effects of heat and mass transfer on mhd free convective flow of maxwell fluid with variable temperature and concentration, *Math. Probl. Eng.* **2021** (2021) 6641835.
31. H. Stehfest, Unsteady natural convection boundary layer heat transfer of fractional Maxwell viscoelastic fluid over a vertical plate, *Commun. ACM* **13**(1) (1970) 47.
32. D. Y. Tzou, *Macro to Micro Scale Heat Transfer*: *The Lagging Behavior* (Taylor and Francis, Washington, 1997).
33. K. A. Abro and I. Khan, MHD flow of fractional Newtonian fluid embedded in a porous medium via Atangana–Baleanu fractional derivatives, *Discrete Contin. Dynam. Syst.-S* **13**(3) (2020) 377–387.
34. N. Iftikhar, D. Baleanu, M. B. Riaz and S. M. Husnine, Heat and mass transfer of natural convective flow with slanted magnetic field via fractional operators, *J. Appl. Comput. Mech.* **6**(SI) (2020) 1613–1636.
35. C. Fetecau, N. A. Shah and D. Vieru, General solutions for hydromagnetic free convection flow over an infinite plate with Newtonian heating, mass diffusion and chemical reaction, *Commun. Theor. Phys.* **68** (2017) 6.